



ENHANCED KNOWLEDGE IN SCIENCES AND
TECHNOLOGY

e-ISSN: 2773-6385

Vol. 4 No. 1 (2024) 298-304

<https://publisher.uthm.edu.my/periodicals/index.php/ekst>

EKST

Crystalline Phase, Microstructure, Optical Properties and Electrical Resistivity in Monovalent Doped $\text{Pr}_{0.75}\text{Na}_{0.2}\text{Ag}_{0.05}\text{Mn}_{1-x}\text{Co}_x\text{O}_3$ ($x = 0 - 0.05$) Manganites

Muhammad Amer Mohd Azizi¹, T. W. Lin¹, Suhadir Shamsuddin^{1*}

¹ Ceramic and Amorphous Group, Department of Physic and Chemistry, Faculty of Applied Sciences and Technology, Universiti Tun Hussien Onn Malaysia, 86400 Pagoh, Johor, Malaysia
Hab Pendidikan Tinggi Pagoh, KM 1, Jalan Panchor, 84600 Pagoh, Muar, Johor, MALAYSIA

*Corresponding Author: suhadir@uthm.edu.my

DOI: <https://doi.org/10.30880/ekst.2024.04.01.034>

Article Info

Received: 27 December 2023

Accepted: 14 January 2024

Available online: 27 July 2024

Keywords

Perovskite, Cobalt, Jahn–Teller.

Abstract

Monovalent doped $\text{Pr}_{0.75}\text{Na}_{0.2}\text{Ag}_{0.05}\text{Mn}_{1-x}\text{Co}_x\text{O}_3$ ($x = 0, 0.02, \text{ and } 0.05$) which prepared by using solid state reaction method have been studied to investigate the effect of crystalline phase, microstructure, and optical properties as well as electrical resistivity using X-ray diffraction (XRD), scanning electron microscope (SEM), Fourier-transform infrared spectroscopy (FTIR) and four-point probe respectively. XRD result showed all samples have been analysis as an orthorhombic structure with *Pnma* space group and the lattice parameter as well as the unit cell volume was observed to be continually decreased with Co content which can be suggest due to the factor of size mismatch between the Co^{3+} ions and Mn^{3+} ions. The morphological study shows the reduction in grain size in the Co-doped manganite samples which indicates that increasement of Co doping can promote growth of grain size and agglomeration. FTIR spectra indicated a shift in the vibration stretching mode towards higher wavenumbers for all samples which can be attributable to the reduction in lattice parameter. The results from the four-point probe analysis showcased a decrease in resistivity with an increasing concentration of Co-doping, suggesting increment charge carrier density and conductivity and providing insights into the electrical properties. As for that, the effect of Co^{3+} ions doped on $\text{Pr}_{0.75}\text{Na}_{0.2}\text{Ag}_{0.05}\text{MnO}_3$ shows a significant result on influencing the crystalline phase, microstructure, optical properties, and electrical resistivity. As for consequences, this study is aimed to elucidate the rules of cobalt doping on influencing the Jahn Teller effect on perovskite manganites.

This is an open access article under the CC BY-NC-SA 4.0 license.



1. Introduction

Comprehensive investigation of manganese oxide with general formula $\text{Re}_{1-x}\text{A}_x\text{MnO}_3$ (Re = a trivalent rare-earth ion, A = a divalent alkali-earth) have been broadly investigated after the discovery of the colossal magnetoresistance (CMR) effect in rare-earth perovskite-type manganites. This attraction of attention is due to their unusual physical properties as well as their possible application such as magnetic sensor at low temperature [1–3]. Subsequent investigation also had proved that monovalent-doped perovskite manganites manifest a substitution of rare earth elements, leading to establishment of a mixed $\text{Mn}^{3+}/\text{Mn}^{4+}$ oxidation state. This substitution induces a detectable transition from a paramagnetic-insulator to a ferromagnetic-metallic phase [4–5]. The exploration of rare earth manganites has received considerable attention, primarily attributed to the presence of charge-ordering (CO) in the compound. CO refers to the ordering of metal ions in different oxidation states, leading to the localization of charge and constraining electron movement from one site to another where this phenomenon contributes to the manifestation of insulating or semiconducting behaviour in the manganite.[6–7]

In particular, research by N. Nasuha Khairuzaman had proved some interesting traits on $\text{Pr}_{0.75}\text{Na}_{0.2}\text{Ag}_{0.05}\text{MnO}_3$ manganites compound. Based on these previous research, the effect of Ag-doped at Na-site of $\text{Pr}_{0.75}\text{Na}_{0.25-y}\text{Ag}_y\text{MnO}_3$ ($0 \leq y \leq 0.10$) manganites, had exhibit metal insulator behaviour transition at $y = 0.05$ suggestively due to the double-exchange (DE) mechanism which had overpowered the effect of Jahn-Teller (JT) effect, while for $y = 0$ and $y = 0.10$ samples had shown an insulating behaviour due to dominant of JT effect [8]. This had proved that by doping Ag at Na site of perovskite structure will alter the JT effect of the sample.

On the other hands, cobalt (Co) emerges as an excellent candidate for doping at the Mn site, given its potential for diverse oxidation states and multiple spin states [9]. Furthermore, the disparities in ionic radius and electronic configuration between Co^{3+} (0.610 Å), Mn^{3+} (0.640 Å), and Mn^{4+} (0.53 Å) add an intriguing dimension to this investigation. This aspect not only alters the Mn^{3+} to Mn^{4+} ratio but also exerts an influence on the CO state, enhancing the complexity and interest of the study [10]. Investigation reported by Srivastava [11] also proved that the critical temperature, T_c of $\text{La}_{0.7}\text{Ca}_{0.3}\text{Mn}_{1-x}\text{Co}_x\text{O}_3$ had been successfully reduced from 260K into 220K due to weakening of double exchange mechanism. Based on investigation by Raveau [6] the results from Co doping into $\text{Pr}_{0.5}\text{Ca}_{0.5}\text{MnO}_3$ had resulted in metal-insulator transition within the compound. Investigation reported by Habibah [2] by increasing of Co content from $y = 0.02$ to $y = 0.05$ on sample $\text{Pr}_{0.75}\text{Na}_{0.25}\text{Mn}_{1-y}\text{Co}_y\text{O}_3$ caused a MI transition to shift to lower temperature which can be suggested due to the weakening of DE mechanism.

However, The Jahn Effect has not been clearly understood. As a consequence, this study scrutinized the impact of chromium (Co) doping on the manganese (Mn) sites within the composition of $\text{Pr}_{0.75}\text{Na}_{0.05}\text{Ag}_{0.05}\text{Mn}_{1-x}\text{Co}_x\text{O}_3$. The investigation extended to exploring the influence of Co on various facets, encompassing structural characteristics, surface morphology, optical attributes, and electrical properties. The selection of Co-doping in this research stems from the intriguing alignment of the Co^{3+} ion possessing an equivalent valence electron configuration as the Mn^{4+} ion, albeit with a smaller ionic radius. Furthermore, the study delved into presenting and discussing pertinent data on density and porosity values.

2. Materials and Methods

All The Co-doped $\text{Pr}_{0.75}\text{Na}_{0.2}\text{Ag}_{0.05}\text{Mn}_{1-x}\text{Co}_x\text{O}_3$ ($x = 0, 0.02, 0.05$) manganite sample have been prepared using solid state reaction methods. A stoichiometric mixture of high purity (>99.99%) Pr_6O_{11} , Na_2CO_3 , Ag_2O , MnO_2 and Co_3O_4 powders were mixed and grinded carefully by using an agate mortar. The process was followed by 24 hours of calcination at 1000°C by utilizing Protherm Furnace Model PLF 130/15 with several intermediate grindings for an hour. The fine powders then being pressed into pellet form with pressure of 5 tons with 13mm diameter. For final preparation process, the pelleted samples were then being sintered at 1200°C for 24 hours.

For sample characterisation, the specimens were finely powdered and subsequently subjected to X-ray diffraction (XRD) analysis utilizing a Bruker D2 Phase Model for crystalline structural characterization. $\text{CuK}\alpha$ radiation was employed at room temperature, and the resolution of 99% was applied to verify the structural composition. Throughout the characterization process, the sample underwent continuous scanning within the range of $20^\circ \leq 2\theta \leq 80^\circ$, with a scanning rate set at $2^\circ/\text{min}$. also had been studied by using X-ray diffraction instruments model Bruker D2 Phase Model. For second sample characterization, Scanning Electron Microscopy model Coxem EM-30AX Plus equipped with energy dispersive X-ray dispersive was used to study the surface morphology of the sample along with elemental composition. After that, the optical properties of sample material have been characterised by utilized FTIR model Agilent Technologies Cary 630. The electrical resistance also had been studied by using four-point probe instruments at room temperature. Archimedes principle have been applied to study the sample density properties whereas there is porosity obtained within using calculations using the standard formula which based on the bulk density, powder density, and also theoretical density.

3. Results and Discussion

Figure 1 displays the powder X-ray diffraction (XRD) patterns for monovalent-doped $\text{Pr}_{0.75}\text{Na}_{0.2}\text{Ag}_{0.05}\text{Mn}_{1-x}\text{Co}_x\text{O}_3$, with varying cobalt (Co) concentrations ($x = 0, 0.02, \text{ and } 0.05$). Analysis of the X-ray diffraction (XRD) patterns revealed that all specimens exhibited crystallization in an orthorhombic crystal structure with a $Pnma$ space group, aligning with findings from a prior investigation [12]. The absence of impurity peaks in the XRD patterns affirms that all discernible peaks pertain to a singular crystalline phase.

The values for lattice parameters, unit cell volume (V), density (D), porosity (%), and resistivity (Ω) for each sample are presented in Table 1. The a-lattice, b-lattice, and c-lattice exhibited a continuous reduction from 5.474 Å, 7.753 Å, and 5.471 Å ($x = 0$) to 5.468 Å, 7.738 Å, and 5.462 Å ($x = 0.05$), respectively. Moreover, the unit cell volume closely followed the trend of lattice parameters, diminishing from 232.19 Å ($x = 0$) to 231.10 Å ($x = 0.05$). The consistent decrease in unit cell volume with Co doping can be suggested due to influence of the substitution of Co^{3+} for Mn^{3+} , resulting in a distortion of the lattice structure due to the differing ionic radii of the two ions. This phenomenon corresponded with previous study which ascribed the smaller ionic radius of Co^{3+} ions (0.610 Å) successfully substitute the larger ionic radius of Mn^{3+} ions (0.640 Å) [13]. At the same time, as the Co concentration increases, the sample resistivity had shown constant reduction from 113.08 Ω ($x=0$), to 106.73 Ω ($x=0.02$), and lastly being decrease to 97.09 Ω ($x=0.05$), inline with the decreasing of lattice parameters.

Table 1 Lattice parameter, unit cell volume (V), density (D), and resistivity (Ω) for the sample $\text{Pr}_{0.75}\text{Na}_{0.2}\text{Ag}_{0.05}\text{Mn}_{1-x}\text{Co}_x\text{O}_3$ ($x = 0.00, 0.02, \text{ and } 0.05$)

Sample	Lattice Parameter (± 0.001)			V (\AA^3)	D (g/cm^3)	Porosity (%)	Resistivity (Ω)
	a (\AA)	b (\AA)	c (\AA)	(± 0.1)	(± 0.01)	(± 0.001)	(± 0.01)
$x = 0$	5.474	7.753	5.471	232.2	5.89	2.343	113.8
$x = 0.02$	5.470	7.747	5.466	231.6	5.60	5.713	106.7
$x = 0.05$	5.468	7.738	5.462	231.1	5.68	5.652	97.09

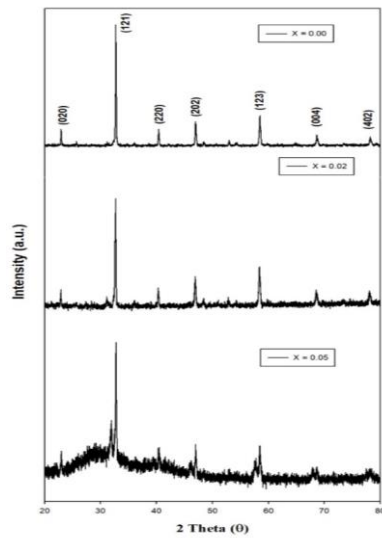


Fig. 1 Powder X-ray diffraction (XRD) pattern of $\text{Pr}_{0.75}\text{Na}_{0.2}\text{Ag}_{0.05}\text{Mn}_{1-x}\text{Co}_x\text{O}_3$ ($x = 0, 0.02, \text{ and } 0.05$) samples

Fig. 2 display an SEM imaging result on all samples with the magnification of 2kX. The SEM images revealed that there are changes of grain size as the Co doping concentration increase, it can also be observe that compactment of grain boundary as the doping concentration increase. This can be suggested that increasement of Co doping can promote growth of grain size and agglomeration. The agglomeration rate of the grain keep increase when the Co concentration increase until at the concentration of Co=0.5 there are very little visible pore. This can indicate that cobalt has been successfully substituted, and it also consistent with SEM EDX which prove the increasement of Co^{3+} being successfully substituted with the Mn^{3+} . In fact, our finding is in agreement with previous study [10]

Fig. 3 illustrates the Energy Dispersive X-ray (EDX) spectrum for all examined samples. The spectrum confirms the presence of all intended elements (Pr, Na, Ag, Co, Mn, O) without any discernible impurities, indicating meticulous sample preparation. Notably, the escalation in the atomic percentage of the Co element suggests the successful unification of Co^{3+} into the samples, with a further increase in atomic percentage for $x = 0.02$ and $x = 0.05$, signifying an augmented concentration of Co doping. Additionally, the weight percentage analysis indicates an elevation in the Mn element, aligning with the notion of smaller ions of Co^{3+} being successfully doped into the Mn^{3+} . Thus, this existences of Co in the samples has proven the changing in SEM image and the unit cell volume stated in XRD result.

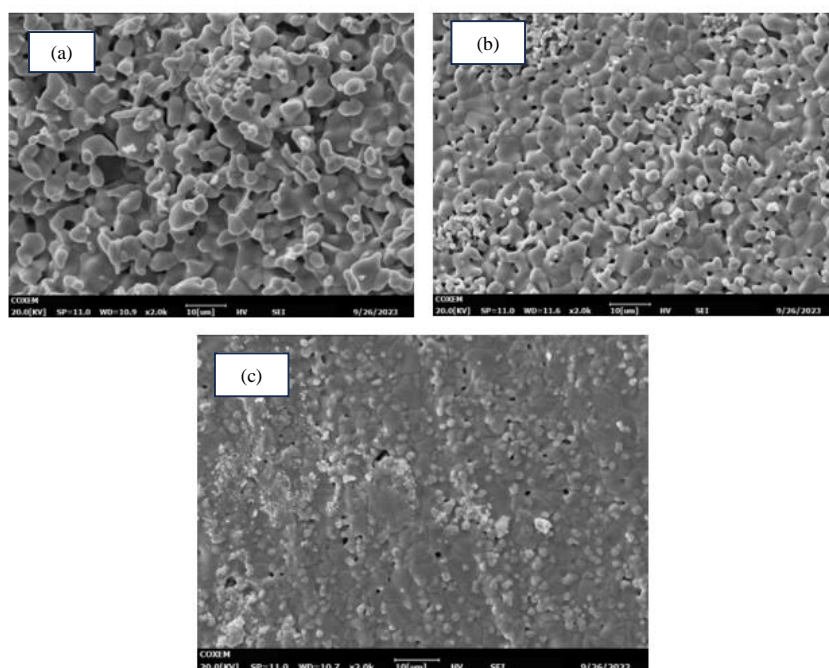


Fig. 2 SEM images with 2kX magnification for $\text{Pr}_{0.75}\text{Na}_{0.2}\text{Ag}_{0.05}\text{Mn}_{1-x}\text{Co}_x\text{O}_3$ (a) $x = 0$, (b) $x = 0.02$ (c) $x = 0.05$

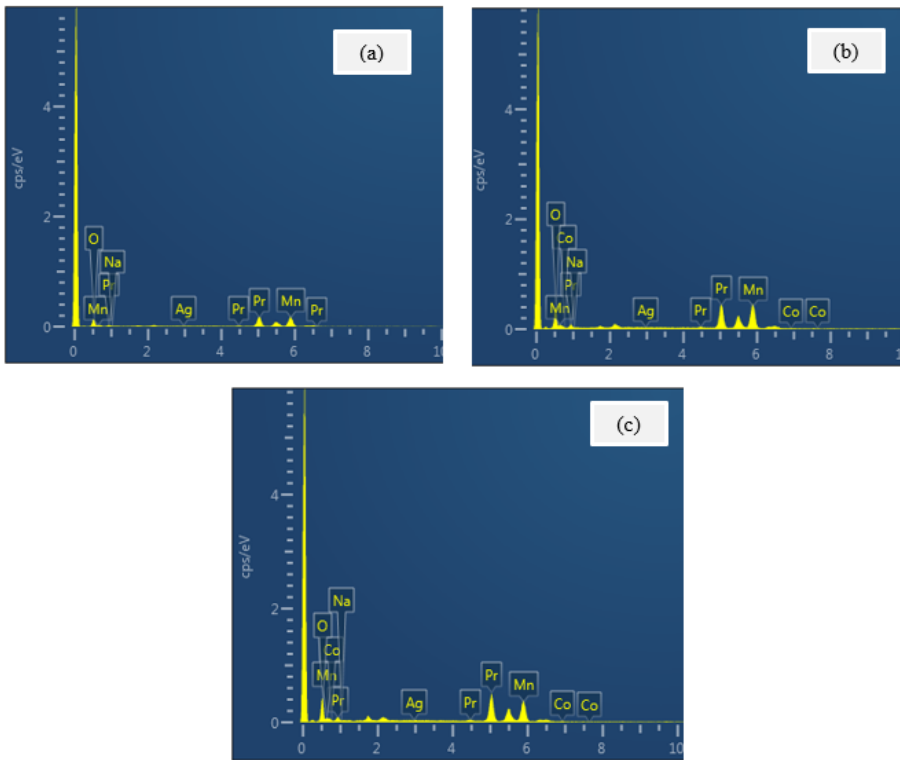


Fig. 3 EDX spectrum for the sample $\text{Pr}_{0.75}\text{Na}_{0.2}\text{Ag}_{0.05}\text{Mn}_{1-x}\text{Co}_x\text{O}_3$ (a) $x = 0$, (b) $x = 0.02$ (c) $x = 0.05$

The FTIR analysis of $\text{Pr}_{0.75}\text{Na}_{0.2}\text{Ag}_{0.05}\text{Mn}_{1-x}\text{Co}_x\text{O}_3$ perovskite manganite from 500cm^{-1} to 1200cm^{-1} was shown in Figure 4. The Fourier Transform Infrared (FTIR) analysis reveals broad hump peaks at 693cm^{-1} and 1021cm^{-1} , along with a distinct absorption peak at 912cm^{-1} . These features signify the presence of robust metal-oxygen bonds in the sample, influenced by either stretching or bending vibration modes [14] [15] [16]. As the concentration of Co-doping increases, there is a notable shift of the absorption peaks towards higher wavenumbers (blue-shift). This shift is indicative of an alteration in the stretching bond length between Mn-O-Mn, attributing it to the disruption of the lattice structure of Mn by the smaller ionic radius of Co, thereby implying a further distortion of the MnO_6 octahedron.

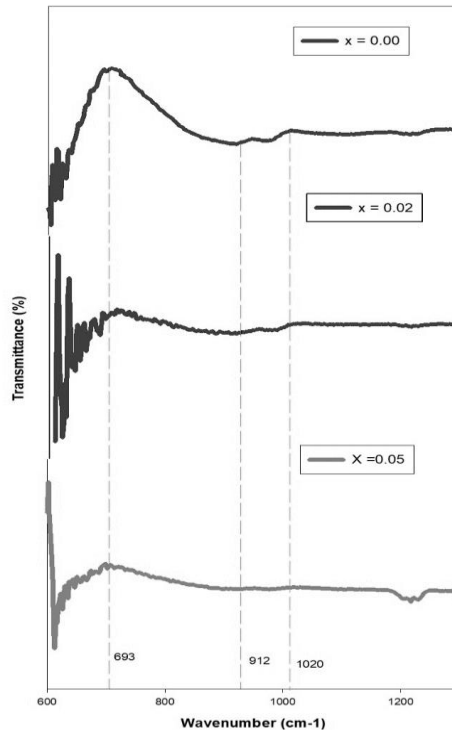


Fig. 4 FTIR analysis of $Pr_{0.75}Na_{0.2}Ag_{0.05}Mn_{1-x}Co_xO_3$ ($x = 0, 0.02, \text{ and } 0.05$) manganite

4. Conclusion

In conclusion, crystalline phase, electrical properties and surface morphology of the monovalent doped of $Pr_{0.75}Na_{0.2}Ag_{0.05}Mn_{1-x}Co_xO_3$ ($x = 0, 0.02, \text{ and } 0.05$) samples have been investigated. Powder X-ray diffraction measurement show that all the synthesized samples were crystallized in the orthorhombic structure with $Pnma$ space group. The increase in Co doping leads to a corresponding reduction in the unit cell volume of the sample. This is attributed to the substitution of the Mn^{3+} ion with the Co^{3+} ion, which possesses a smaller ionic radius, triggering lattice distortion in the samples. SEM analysis reveals a discernible augmentation in grain size and the development of grain boundary compartments with escalating Co doping concentrations, indicative of a pronounced influence fostering both grain growth and agglomeration. The escalating agglomeration rate persists with increasing Co concentration, culminating at $Co=0.5$, where a paucity of discernible pores is noted. This observation implies the efficacious substitution of cobalt, corroborated by SEM EDX results affirming the heightened presence of Co^{3+} substituting for Mn^{3+} . The four-point probe analysis illustrated a decrease in resistivity, signifying alterations in the CO state influenced by the presence of Co-doping. On the other hand, the FTIR analysis of $Pr_{0.75}Na_{0.2}Ag_{0.05}Mn_{1-x}Co_xO_3$ ($x = 0, 0.02, \text{ and } 0.05$) perovskite manganite reveals distinctive absorption peaks, with a notable blue-shift in absorption peaks at higher wavenumbers as the concentration of Co-doping increases, suggesting a disruption in the lattice structure of MnO_6 octahedra. As a final assumption from result discussion, it has been concluded that Co dopin from this study that by doping Co into $Pr_{0.75}Na_{0.2}Ag_{0.05}Mn_{1-x}Co_xO_3$ ($x = 0, 0.02, \text{ and } 0.05$), the Jahn Teller effect have been weakened.

Acknowledgement

Thanks to all laboratories assistance from material and nanotechnologies laboratories. Thanks to Ceramic and Amorphous Group, Faculty of Applied Sciences and Technology, Pagoh Higher Education Hub, University Tun Hussein Onn Malaysia (UTHM)

Commented [MABZ1]: Use Acknowledgement Style

Conflict of Interest

There are no conflict interests regarding the publication of the paper.

Author Contribution

The authors confirm contribution to the paper as follows: **study conception and design, data collection, methodology, analysis and interpretation of results:** Muhammad Amer Mohd Azizi, T.W.Lin and Suhadir Shamsuddin. All authors reviewed the results and approved the final version of the manuscript.

References

- [1] Zawawi, R. A., Ibrahim, N., & Shamsuddin, S. (2018). Enhancement of double-exchange mechanism in charge-ordered $\text{Pr}_{0.75}\text{Na}_{0.25}\text{MnO}_3$ ceramic by Cr doped at Mn-site. *International Journal Current Science, Engineering and Technology*, 1(S1), 101-106.
- [2] Ab Mannan, Nurhabibah Nabilah, et al. "Crystalline phase, surface morphology and electrical properties of monovalent-doped $\text{Nd}_{0.75}\text{Na}_{0.25}\text{Mn}_{1-x}\text{Co}_x\text{O}_3$ manganites." *Journal of Science and Technology* 9.3 (2017).
- [3] Zawawi, R. A., Khairulzaman, N. N., Shamsuddin, S., & Ibrahim, N. (2018). Comparative Study on Structural, Electrical Transport and Magnetic Properties of Cr-Doped in Charge-Ordered. *International Journal of Engineering & Technology*, 7(4.30), 75-79.
- [4] Debnath, J. C., Zeng, R., Kim, J. H., & Dou, S. X. (2011). "Multifunctionality from coexistence of large magnetoresistance and magnetocaloric effect in $\text{La}_{0.7}\text{Ca}_{0.3}\text{MnO}_3$," AIP Conf. Proc., 1347, 278–281.
- [5] Thaljaoui, R., Boujelben, W., Pėkała, M., Pėkała, K., Mucha, J., & Cheikhrouhou, A. (2013). "Structural, magnetic and transport study of monovalent Na-doped manganite $\text{Pr}_{0.55}\text{Na}_{0.05}\text{Sr}_{0.4}\text{MnO}_3$," J. Alloys Compd., 558, 236–243.
- [6] Raveau, B., Martin, C., Maignan, A., Hervieu, M., & Mahendiran, R. (2000). "Mn-site doping in colossal magnetoresistance manganites" in *Physica C: Superconductivity*, 341, 711-714.
- [7] Liu, Y., Kong, H., & Zhu, C. F. (2007). "Coexistence of charge ordering and ferromagnetism in $\text{Nd}_{0.5}\text{Ca}_{0.5}\text{Mn}_{1-x}\text{Co}_x\text{O}_3$ ($x \leq 0.1$)" in *Journal of Alloys Compound*, 439, 33–36.
- [8] Khairulzaman, N. N., Shamsuddin, S., & Ibrahim, N. (2020). Effect of Ag-doped on electrical transport properties in $\text{Pr}_{0.75}\text{Na}_{0.25}\text{MnO}_3$ manganites. *Journal of Advanced Research in Dynamical and Control Systems*, 12(2), 759-765.
- [9] Modaresi, N., Kameli, P., & Salamati, H. (2014). "Impact of Co Doping on Magnetic and Electrical Properties of $\text{La}_{0.5}\text{Ca}_{0.5}\text{Mn}_{1-x}\text{Co}_x\text{O}_3$ ($0 \leq x \leq 0.05$) Manganites" in *Journal of Magnetism and Magnetic Materials*, 365, 107–114.
- [10] Huang, X., Chen, W., Wu, W., Zhou, Y., Wu, J., Wang, Q., & Chen, Y. (2016). "Effect of Co^{3+} Substitution on the Structure and Magnetic Properties of $\text{La}_{0.6}\text{Ca}_{0.4}\text{MnO}_3$ " in *Journal of Material Science: Materials in Electronics*, 27(5), 5395–5402.
- [11] Srivastava, C. M., Banerjee, S., Gundurao, T. K., Nigam, A. K., & Bahadur, D. (2003). "Evidence of Spin Transition and Charge Order in Cobalt Substituted $\text{La}_{0.7}\text{Ca}_{0.3}\text{MnO}_3$ " in *Journal of Physics: Condensed Matter*, 15, 2375–2388.
- [12] Abdullah, H., & Halim, S. A. (2010). "Disorder Phenomena in Nd-doped $(\text{Pr}_{1-x}\text{Nd}_x)_0.67\text{Ba}_{0.33}\text{MnO}_3$ Manganites" in *Sains Malaysiana*, 39(1), 93–98.
- [13] Shannon, R. D. (2010). "Revised Effective Ionic Radii and Systematic Studies of Interatomic Distances in Halides and Chalcogenides" in *Acta Crystallographica*, A32, 751-767.
- [14] B. Singh, P. Singh, S. Siddiqui, D. Singh and M. Gupta, "Wastewater treatment using Fe-doped perovskite manganites by photocatalytic degradation of methyl orange, crystal violet and indigo carmine dyes in tungsten bulb/sunlight," *Journal of Rare Earths*, vol. 41, no.10.1016/j.jre.2022.09.010, pp. 1311-1322, 2023.
- [15] H. Nayak and B. Padhi, "Degradation of methylene blue using Ca-doped LaMnO_3 as a photocatalyst under visible light irradiation," *Results in Chemistry*, vol. 6, no.10.1016/i.rechem.2023.101104. p. 101104. 2023
- [16] Yunus, Z. M., & Azaha, N. A. N. (2021). Jackfruit Seeds Starch-Based Coagulant for Synthetic Textile Wastewater Remediation. *Enhanced Knowledge in Sciences and Technology*, 1(2), 72-80.